Hindawi Publishing Corporation
Journal of Applied Mathematics
Volume 2013, Article ID 284208, 7 pages
http://dx.doi.org/10.1155/2013/284208

Research Article

Natural Frequencies of Shear Deformable Plates by Polyharmonic Splines

A. J. M. Ferreira[1,2] and A. M. Zenkour[2,3]

[1] *Faculdade de Engenharia da Universidade do Porto, Porto, Portugal*
[2] *Department of Mathematics, Faculty of Science, King Abdulaziz University, P.O. Box 80203, Jeddah 21589, Saudi Arabia*
[3] *Department of Mathematics, Faculty of Science, Kafr El-Sheikh University, Kafr El-Sheikh 33516, Egypt*

Correspondence should be addressed to A. J. M. Ferreira; ferreira@fe.up.pt

Received 10 July 2013; Accepted 16 September 2013

Academic Editor: Carla Roque

We use the third-order shear deformation theory and a collocation technique with polyharmonic splines to predict natural frequencies of moderately thick isotropic plates. The natural frequencies of vibration are computed for various plates and compared with some available published results. Through numerical experiments, the capability and efficiency of the present method for eigenvalue problems are demonstrated, and the numerical accuracy and convergence are thoughtfully examined.

1. Introduction

Radial basis functions (RBFs) have recently proved to be an excellent technique for interpolating data and functions. A radial basis function $\phi(\|x - x_j\|)$ can be considered a spline that depends on the Euclidean distance between distinct data centers x_j, $j = 1, 2, \ldots, N \in \mathbb{R}^n$, also called nodal or collocation points. Not only RBFs are adequate to scattered data approximation and in general to interpolation theory, as proposed by Hardy [1], but also excellent for solving partial differential equations (PDEs) as first introduced by Kansa [2].

Kansa proposed an unsymmetric RBF collocation method based upon multiquadric interpolation functions, in which the shape parameter is considered to be variable across the problem domain. The distribution of the shape parameter is obtained by an optimization approach, in which the value of the shape parameter is assumed to be proportional to the curvature of the unknown solution of the original partial differential equation. In this way, it is possible to reduce the condition number of the matrix at the expense of implementing an additional iterative algorithm. In the present work, we will implement the unsymmetric global collocation method in a form that is independent of this shape parameter based on unshifted polyharmonic splines. In some respect this can be seen as a more stable form than multiquadrics.

Structures composed of laminated materials are among the most important structures used in modern engineering and, especially, in the aerospace industry. Such lightweight structures are also being increasingly used in civil, mechanical, and transportation engineering applications. The rapid increase of the industrial use of these structures has necessitated the development of new analytical and numerical tools that are suitable for the analysis and study of the mechanical behavior of such structures. The behavior of structures composed of advanced composite materials is considerably more complicated than for isotropic ones. The strong influences of anisotropy, the transverse stresses through the thickness of a laminate, and the stress distributions at interfaces are among the most important factors that affect the general performance of such structures. The use of shear deformation theories has been the topic of intensive research, as in [7–19], among many others.

The analysis of laminated plates by finite element methods is now considerably established. The use of alternative methods such as the meshless methods based on radial basis functions is attractive due to the absence of a mesh and the ease of collocation methods. The use of radial basis function for the analysis of structures and materials has been previously studied by numerous authors [20–31]. More recently the authors have applied RBFs to the static deformations of composite beams and plates [32–35]. Recent meshless techniques were discussed in [36–42].

In this paper the use of radial basis functions to isotropic and composite plates using a third-order shear deformation theory is investigated. The quality of the present method in predicting free vibrations of isotropic and laminated composite plates is compared and discussed with other methods in some numerical examples.

2. The Radial Basis Function Method

2.1. The Eigenproblem. Radial basis functions (RBF) approximations are grid-free numerical schemes that can exploit accurate representations of the boundary, are easy to implement, and can be spectrally accurate [43, 44].

In this section the formulation of a global unsymmetrical collocation RBF-based method to compute eigenvalues of elliptic operators is presented.

Consider a linear elliptic partial differential operator L and a bounded region Ω in $\mathbb{R}^n$ with some boundary $\partial\Omega$. The eigenproblem looks for eigenvalues (λ) and eigenvectors ($\mathbf{u}$) that satisfy

$$\begin{aligned} L\mathbf{u} + \lambda\mathbf{u} &= 0 \quad \text{in } \Omega, \\ L_B\mathbf{u} &= 0 \quad \text{on } \partial\Omega, \end{aligned} \tag{1}$$

where L_B is a linear boundary operator. The eigenproblem of (1) is replaced by a finite-dimensional eigenvalue problem, based on RBF approximations.

The operator L is approximated by a matrix that incorporates the boundary conditions and then solve the eigenvalues and eigenvectors of this matrix by standard techniques.

2.2. Radial Basis Functions. The radial basis function (ϕ) approximation of a function ($\mathbf{u}$) is given by

$$\tilde{\mathbf{u}}(\mathbf{x}) = \sum_{i=1}^{N} \alpha_i \phi\left(\|x - y_i\|_2\right), \quad \mathbf{x} \in \mathbb{R}^n, \tag{2}$$

where y_i, $i = 1, \ldots, N$ is a finite set of distinct points (centers) in $\mathbb{R}^n$. The coefficients α_i are calculated so that $\tilde{\mathbf{u}}$ satisfies some boundary conditions. Although many other functions could be used, as illustrated by several authors [1, 2, 45], here we use unshifted polyharmonic splines in the form

$$\phi(r) = r^{2m+1}, \quad m \in Z, \tag{3}$$

where the Euclidean distance r is real and nonnegative.

Considering N distinct interpolations, and knowing $u(x_j)$, $j = 1, 2, \ldots, N$, we find α_i by the solution of a $N \times N$ linear system $\mathbf{A}\underline{\alpha} = \mathbf{u}$, where $\mathbf{A} = [\phi(\|x - y_i\|_2)]_{N\times N}$, $\underline{\alpha} = [\alpha_1, \alpha_2, \ldots, \alpha_N]^T$ and $\mathbf{u} = [u(x_1), u(x_2), \ldots, u(x_N)]^T$. The RBF interpolation matrix A is positive definite for some RBFs [46] but in general provides ill-conditioned systems. This ill-conditioning problem is due to full matrices produced by the collocation method and worsens with the increase of number of nodes. However it was shown by Schaback that the more ill-conditioned the problem the better the solution, until a flatness of the function occurs. In our numerical experiments this ill-conditioning did not produce any inconvenience to quality of solution.

2.3. Solution of the Eigenproblem. We follow a simple scheme for the solution of the eigenproblem (1). We consider N_I nodes in the interior of the domain and N_B nodes on the boundary, with $N = N_I + N_B$.

We denote interpolation points by $x_i \in \Omega, i = 1, \ldots, N_I$ and $x_i \in \partial\Omega, i = N_I + 1, \ldots, N$. For the interior points we have that

$$\sum_{i=1}^{N} \alpha_i L\phi\left(\|x - y_i\|_2\right) = \lambda\tilde{\mathbf{u}}\left(x_j\right), \quad j = 1, 2, \ldots, N_I \tag{4}$$

or

$$L^I\underline{\alpha} = \lambda\tilde{\mathbf{u}}^I, \tag{5}$$

where

$$L^I = \left[L\phi\left(\|x - y_i\|_2\right)\right]_{N_I\times N}, \tag{6}$$

For the boundary conditions we have

$$\sum_{i=1}^{N} \alpha_i L_B\phi\left(\|x - y_i\|_2\right) = 0, \quad j = N_I + 1, \ldots, N \tag{7}$$

or

$$\mathbf{B}\underline{\alpha} = 0. \tag{8}$$

Therefore we can write a finite-dimensional problem as a generalized eigenvalue problem

$$\begin{bmatrix} L^I \\ \mathbf{B} \end{bmatrix} \underline{\alpha} = \lambda \begin{bmatrix} \mathbf{A}^I \\ \mathbf{0} \end{bmatrix} \underline{\alpha}, \tag{9}$$

where

$$\begin{aligned} \mathbf{A}^I &= \phi\left[\left(\left\|x_{N_I} - y_j\right\|_2\right)\right]_{N_I\times N}, \\ \mathbf{B}^I &= L_B\phi\left[\left(\left\|x_{N_I+1} - y_j\right\|_2\right)\right]_{N_B\times N}. \end{aligned} \tag{10}$$

3. Third-Order Theory

The displacement field for the third-order shear deformation theory of Hardy [1] is obtained as

$$\begin{aligned} u(x, y, z, t) &= u_0(x, y, t) + z\theta_x(x, y, t) - \frac{4}{3h^2}z^3\left(\theta_x + \frac{\partial w}{\partial x}\right), \\ v(x, y, z, t) &= v_0(x, y, t) + z\theta_y(x, y, t) - \frac{4}{3h^2}z^3\left(\theta_y + \frac{\partial w}{\partial y}\right), \\ w(x, y, z, t) &= w_0(x, y, t), \end{aligned} \tag{11}$$

where u and v are the in-plane displacements at any point (x, y, z), u_0,v_0 denote the in-plane displacement of the point $(x, y, 0)$ on the midplane, w is the deflection, and θ_x and θ_y are the rotations of the normals to the midplane about the y- and x-axes, respectively.

The strain-displacement relationships are given as

$$\begin{Bmatrix} \epsilon_{xx} \\ \epsilon_{yy} \\ \gamma_{xy} \\ \gamma_{xz} \\ \gamma_{yz} \end{Bmatrix} = \begin{Bmatrix} \dfrac{\partial u}{\partial x} \\ \dfrac{\partial v}{\partial y} \\ \dfrac{\partial u}{\partial y} + \dfrac{\partial v}{\partial x} \\ \dfrac{\partial u}{\partial z} + \dfrac{\partial w}{\partial x} \\ \dfrac{\partial v}{\partial z} + \dfrac{\partial w}{\partial y} \end{Bmatrix}. \tag{12}$$

Therefore strains can be expressed as

$$\begin{gathered} \begin{Bmatrix} \epsilon_{xx} \\ \epsilon_{yy} \\ \gamma_{xy} \end{Bmatrix} = \begin{Bmatrix} \epsilon_{xx}^{(0)} \\ \epsilon_{yy}^{(0)} \\ \gamma_{xy}^{(0)} \end{Bmatrix} + z \begin{Bmatrix} \epsilon_{xx}^{(1)} \\ \epsilon_{yy}^{(1)} \\ \gamma_{xy}^{(1)} \end{Bmatrix} + z^3 \begin{Bmatrix} \epsilon_{xx}^{(3)} \\ \epsilon_{yy}^{(3)} \\ \gamma_{xy}^{(3)} \end{Bmatrix}, \\ \begin{Bmatrix} \gamma_{xz} \\ \gamma_{yz} \end{Bmatrix} = \begin{Bmatrix} \gamma_{xz}^{(0)} \\ \gamma_{yz}^{(0)} \end{Bmatrix} + z^2 \begin{Bmatrix} \gamma_{xz}^{(2)} \\ \gamma_{yz}^{(2)} \end{Bmatrix}, \end{gathered} \tag{13}$$

where

$$\begin{gathered} \begin{Bmatrix} \epsilon_{xx}^{(0)} \\ \epsilon_{yy}^{(0)} \\ \gamma_{xy}^{(0)} \end{Bmatrix} = \begin{Bmatrix} \dfrac{\partial u_0}{\partial x} \\ \dfrac{\partial v_0}{\partial y} \\ \dfrac{\partial u_0}{\partial y} + \dfrac{\partial v_0}{\partial x} \end{Bmatrix}, \\ \begin{Bmatrix} \epsilon_{xx}^{(1)} \\ \epsilon_{yy}^{(1)} \\ \gamma_{xy}^{(1)} \end{Bmatrix} = \begin{Bmatrix} \dfrac{\partial \theta_x}{\partial x} \\ \dfrac{\partial \theta_y}{\partial y} \\ \dfrac{\partial \theta_x}{\partial y} + \dfrac{\partial \theta_y}{\partial x} \end{Bmatrix}, \\ \begin{Bmatrix} \epsilon_{xx}^{(3)} \\ \epsilon_{yy}^{(3)} \\ \gamma_{xy}^{(3)} \end{Bmatrix} = -c_1 \begin{Bmatrix} \dfrac{\partial \theta_x}{\partial x} + \dfrac{\partial^2 w_0}{\partial x^2} \\ \dfrac{\partial \theta_y}{\partial y} + \dfrac{\partial^2 w_0}{\partial y^2} \\ \dfrac{\partial \theta_x}{\partial y} + \dfrac{\partial \theta_y}{\partial x} + 2\dfrac{\partial^2 w_0}{\partial x \partial y} \end{Bmatrix}, \\ \begin{Bmatrix} \gamma_{xz}^{(0)} \\ \gamma_{yz}^{(0)} \end{Bmatrix} = \begin{Bmatrix} \dfrac{\partial w_0}{\partial x} + \theta_x \\ \dfrac{\partial w_0}{\partial y} + \theta_y \end{Bmatrix}; \qquad \begin{Bmatrix} \gamma_{xz}^{(2)} \\ \gamma_{yz}^{(2)} \end{Bmatrix} = -c_2 \begin{Bmatrix} \dfrac{\partial w_0}{\partial x} + \theta_x \\ \dfrac{\partial w_0}{\partial y} + \theta_y \end{Bmatrix} \end{gathered} \tag{14}$$

and $c_1 = 4/3h^2$, $c_2 = 3c_1$.

A laminate can be manufactured from orthotropic layers (or plies) of preimpregnated unidirectional fibrous composite materials. Neglecting σ_z for each layer, the stress-strain relations in the fiber local coordinate system can be expressed as

$$\begin{Bmatrix} \sigma_1 \\ \sigma_2 \\ \tau_{12} \\ \tau_{23} \\ \tau_{31} \end{Bmatrix} = \begin{bmatrix} Q_{11} & Q_{12} & 0 & 0 & 0 \\ Q_{12} & Q_{22} & 0 & 0 & 0 \\ 0 & 0 & Q_{33} & 0 & 0 \\ 0 & 0 & 0 & Q_{44} & 0 \\ 0 & 0 & 0 & 0 & Q_{55} \end{bmatrix} \begin{Bmatrix} \varepsilon_1 \\ \varepsilon_2 \\ \gamma_{12} \\ \gamma_{23} \\ \gamma_{31} \end{Bmatrix}, \tag{15}$$

where subscripts 1 and 2 are, respectively, the fiber and the normal to fiber in-plane directions, 3 is the direction normal to the plate, and the reduced stiffness components, Q_{ij}, are given by

$$\begin{gathered} Q_{11} = \frac{E_1}{1 - \nu_{12}\nu_{21}} \qquad Q_{22} = \frac{E_2}{1 - \nu_{12}\nu_{21}} \\ Q_{12} = \nu_{21} Q_{11} \qquad Q_{33} = G_{12} \\ Q_{44} = G_{23} \qquad Q_{55} = G_{31} \\ \nu_{21} = \nu_{12} \frac{E_2}{E_1}, \end{gathered} \tag{16}$$

in which E_1, E_2, ν_{12}, G_{12}, G_{23}, and G_{31} are materials properties of the lamina.

By performing adequate coordinate transformation, the stress-strain relations in the global x-y-z coordinate system can be obtained as

$$\begin{Bmatrix} \sigma_{xx} \\ \sigma_{yy} \\ \tau_{xy} \\ \tau_{yz} \\ \tau_{zx} \end{Bmatrix} = \begin{bmatrix} \overline{Q}_{11} & \overline{Q}_{12} & \overline{Q}_{16} & 0 & 0 \\ \overline{Q}_{12} & \overline{Q}_{22} & \overline{Q}_{26} & 0 & 0 \\ \overline{Q}_{16} & \overline{Q}_{26} & \overline{Q}_{66} & 0 & 0 \\ 0 & 0 & 0 & \overline{Q}_{44} & \overline{Q}_{45} \\ 0 & 0 & 0 & \overline{Q}_{45} & \overline{Q}_{55} \end{bmatrix} \begin{Bmatrix} \varepsilon_{xx} \\ \varepsilon_{yy} \\ \gamma_{xy} \\ \gamma_{yz} \\ \gamma_{zx} \end{Bmatrix}. \tag{17}$$

The third-order theory of Hardy [15, 16] satisfies zero transverse shear stresses on the bounding planes.

The equations of motion of the third-order theory are derived from the principle of virtual displacements:

$$
\begin{aligned}
&\frac{\partial N_{xx}}{\partial x}+\frac{\partial N_{xy}}{\partial y}=I_0\frac{\partial^2 u_0}{\partial t^2}+J_1\frac{\partial^2\theta_x}{\partial t^2}-c_1 I_3\frac{\partial^2}{\partial t^2}\left(\frac{\partial w_0}{\partial x}\right),\\
&\frac{\partial N_{xy}}{\partial x}+\frac{\partial N_{yy}}{\partial y}=I_0\frac{\partial^2 v_0}{\partial t^2}+J_1\frac{\partial^2\theta_y}{\partial t^2}-c_1 I_3\frac{\partial^2}{\partial t^2}\left(\frac{\partial w_0}{\partial y}\right),\\
&\frac{\partial \overline{Q}_x}{\partial x}+\frac{\partial \overline{Q}_y}{\partial y}+c_1\left(\frac{\partial^2 P_{xx}}{\partial x^2}+2\frac{\partial^2 P_{xy}}{\partial x\,\partial y}+\frac{\partial^2 P_{yy}}{\partial y^2}\right)+q\\
&\quad=I_0\frac{\partial^2 w_0}{\partial t^2}-c_1 I_6\frac{\partial^2}{\partial t^2}\left(\frac{\partial^2 w_0}{\partial x^2}+\frac{\partial^2 w_0}{\partial y^2}\right)\\
&\qquad+c_1\left[I_3\frac{\partial^2}{\partial t^2}\left(\frac{\partial u_0}{\partial x}+\frac{\partial v_0}{\partial y}\right)+J_4\frac{\partial^2}{\partial t^2}\left(\frac{\partial \theta_x}{\partial x}+\frac{\partial \theta_y}{\partial y}\right)\right],\\
&\frac{\partial \overline{M}_{xx}}{\partial x}+\frac{\partial \overline{M}_{xy}}{\partial y}-\overline{Q}_x=\frac{\partial^2}{\partial t^2}\left(J_1 u_0+K_2\theta_x-c_1 J_4\frac{\partial w_0}{\partial x}\right),\\
&\frac{\partial \overline{M}_{xy}}{\partial x}+\frac{\partial \overline{M}_{yy}}{\partial y}-\overline{Q}_y=\frac{\partial^2}{\partial t^2}\left(J_1 v_0+K_2\theta_y-c_1 J_4\frac{\partial w_0}{\partial y}\right),
\end{aligned}
\tag{18}
$$

where q is the external distributed load and with

$$
\begin{aligned}
&\overline{M}_{\alpha\beta}=M_{\alpha\beta}-c_1 P_{\alpha\beta};\qquad \overline{Q}_\alpha=Q_\alpha-c_2 R_\alpha,\\
&I_i=\sum_{k=1}^{N}\int_k^{k+1}\rho^{(k)}(z)^i dz,\quad (i=0,1,2,\ldots,6),\\
&J_i=I_i-c_1 I_{i+2}\ (i=1,4),\\
&K_2=I_2-2c_1 I_4+c_1^2 I_6,\qquad c_1=\frac{4}{3h^2},\qquad c_2=4h^2=3c_1,
\end{aligned}
\tag{19}
$$

where α,β take the symbols x, y. The resultants (N_{xx}, N_{yy}, N_{xy}) denote the in-plane force resultants, (M_{xx}, M_{yy}, M_{xy}) the moment resultants, (Q_x, Q_y) the shear resultants and (P_{xx}, P_{yy}, P_{xy}) and (R_x, R_y) denote the higher-order stress resultants:

$$
\begin{aligned}
&\begin{Bmatrix} N_{\alpha\beta}\\ M_{\alpha\beta}\\ P_{\alpha\beta}\end{Bmatrix}=\int_{-h/2}^{h/2}\sigma_{\alpha\beta}\begin{Bmatrix}1\\ z\\ z^3\end{Bmatrix}dz,\\
&\begin{Bmatrix} Q_\alpha\\ R_\alpha\end{Bmatrix}=\int_{-h/2}^{h/2}\sigma_{\alpha z}\begin{Bmatrix}1\\ z^2\end{Bmatrix}dz,
\end{aligned}
\tag{20}
$$

where α,β take the symbols x, y.

If needed, the first-order shear deformation theory equations are readily obtained from the third-order equations, just by putting $c_1 = 0$.

4. Numerical Examples

The eigenvalues presented in this problem are expressed in terms of the nondimensional frequency parameter $\lambda = (\omega b^2/\pi^2)(\rho t/D)^{1/2}$. Unlike first-order shear deformation theories the present approach does not incorporate shear correction factors in the constitutive matrix. The Poisson ratio, ν, is taken to be 0.3 throughout the present problem. Figure 1 illustrates the grid scheme for 11×11 points.

In Tables 1, 2, 3, 4, 5, and 6 we compare the present results with those of Liew et al. [3]. We consider here simply supported (SSSS) and clamped (CCCC) boundary conditions in all edges, thin and thick plates and square and rectangular plates. The results obtained in Tables 1 to 6 show that the present method presents very close results to those proposed by Liew et al. [3]. However, for thin plates we need more

Table 1: Convergence study of frequency parameters, $\lambda = (\omega b^2/\pi^2)(\rho t/D)^{1/2}$ for rectangular isotropic plates with SSSS boundaries, $h/a = 0.001, b/a = 1.0$.

Mode	$N = 21$	$N = 25$	$N = 30$	Liew et al. [3]
1	2.0146	2.0089	2.0087	2.0000
2	5.0630	5.0343	5.0218	5.0000
3	5.0644	5.0371	5.0255	5.0000
4	8.1648	8.0717	8.0508	7.9999
5	9.8773	9.9908	10.0138	9.9998
6	10.2520	10.2462	10.0472	9.9998
7	12.7965	12.9815	13.0339	12.9997
8	12.8308	13.1027	13.0579	12.9997

Table 2: Convergence study of frequency parameters, $\lambda = (\omega b^2/\pi^2)(\rho t/D)^{1/2}$ for rectangular isotropic plates with SSSS boundaries, $h/a = 0.2, b/a = 1.0$.

Mode	$N = 11$	$N = 15$	$N = 21$	Liew et al. [3]
1	1.7725	1.7700	1.7688	1.7659
2	3.8769	3.8717	3.8698	3.8576
3	3.8770	3.8717	3.8699	3.8576
4	5.6201	5.6063	5.6009	5.5729
5	6.5939	6.6093	6.6149	6.5809
6	6.6098	6.6127	6.6153	6.5809
7	8.0235	8.0092	8.0044	7.9470
8	8.0250	8.0099	8.0046	7.9470

Table 3: Convergence study of frequency parameters, $\lambda = (\omega b^2/\pi^2)(\rho t/D)^{1/2}$ for rectangular isotropic plates with SSSS boundaries, $h/a = 0.001, b/a = 2.5$.

Mode	$N = 21$	$N = 25$	$N = 30$	Liew et al. [3]
1	1.2528	1.1294	1.1511	1.1600
2	1.7969	1.5886	1.6694	1.6400
3	3.5791	2.4060	2.4977	2.4400
4	4.1586	2.8928	3.7214	3.5600
5	4.1586	4.5265	4.4835	4.1600
6	6.1938	5.4430	5.1762	4.6400
7	6.2026	5.7588	7.0559	5.0000
8	6.2026	6.4153	7.5293	5.4399

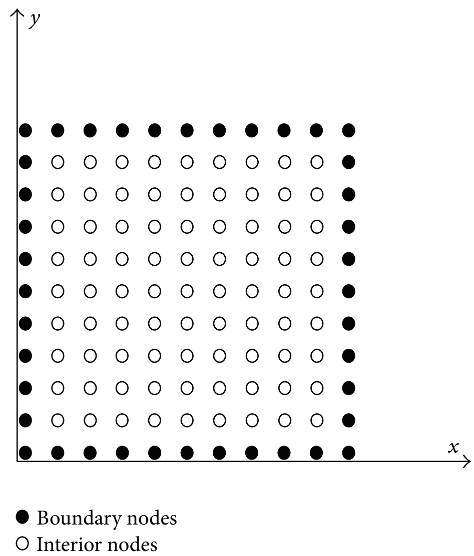

Figure 1: 11 × 11 regular grid for discretization of the square laminated plate.

Table 4: Convergence study of frequency parameters, $\lambda = (\omega b^2/\pi^2)(\rho t/D)^{1/2}$ for rectangular isotropic plates with SSSS boundaries, $h/a = 0.2, b/a = 2.5$.

Mode	$N = 11$	$N = 15$	$N = 21$	Liew et al. [3]
1	1.0699	1.0722	1.0732	1.0741
2	1.4836	1.4789	1.4702	1.4768
3	2.1267	2.1114	2.1041	2.1059
4	2.9901	2.9429	2.9328	2.9145
5	3.3120	3.3224	3.3288	3.3191
6	3.6449	3.6403	3.6375	3.6306
7	4.0418	3.9265	3.9239	3.8576
8	4.1796	4.1508	4.1451	4.1281

Table 5: Convergence study of frequency parameters, $\lambda = (\omega b^2/\pi^2)(\rho t/D)^{1/2}$ for rectangular isotropic plates with CCCC boundaries, $h/a = 0.001, b/a = 1.0$.

Mode	$N = 15$	$N = 21$	$N = 25$	Liew et al. [3]
1	3.9078	3.7202	3.6892	3.6460
2	8.5057	7.7031	7.5817	7.4362
3	8.5057	7.7032	7.5818	7.4362
4	14.7680	11.9358	11.4953	10.9643
5	15.8127	13.7424	13.5536	13.3315
6	17.1194	14.0909	13.7236	13.3947
7	25.6747	18.6394	17.7457	16.7173
8	25.6747	18.6396	17.7458	16.7173

Table 6: Convergence study of frequency parameters, $\lambda = (\omega b^2/\pi^2)(\rho t/D)^{1/2}$ for rectangular isotropic plates with CCCC boundaries, $h/a = 0.2, b/a = 1.0$.

Mode	$N = 11$	$N = 15$	$N = 21$	Liew et al. [3]
1	2.5935	2.5956	2.5976	2.6803
2	4.5153	4.5295	4.5366	4.6744
3	4.5153	4.5295	4.5366	4.6744
4	6.0888	6.1042	6.1166	6.2748
5	6.9553	6.9909	7.0045	7.1481
6	7.0281	7.0730	7.0833	7.2466
7	8.2813	8.3096	8.3290	8.4803
8	8.2813	8.3096	8.3290	8.4803

points than in thick plates in order to get convergent and accurate frequencies. The reason for this behaviour lies in the worse conditioning of thin plates. In Liew et al. [3] thin plates also showed slower convergence.

In Tables 7 and 8 we analyse thin and thick plates for SSSS and CCCC boundaries. Present results are compared with classical theory of Leissa [4], first-order theory of Dawe [5], and orthogonal polynomials of Liew et al. [3]. The present method shows very accurate results when compared to Liew et al. [3] and FSDT of Dawe [5], for both SSSS and CCCC boundary conditions.

5. Conclusions

Radial basis functions are increasingly popular in the analysis of science and engineering problems.

In this paper, we use the third-order shear deformation theory and a collocation technique with polyharmonic splines to predict natural frequencies of moderately thick isotropic plates. The natural frequencies of vibration are computed for various plates and compared with some available published results. The formulation for higher-order plates and their interpolation with polyharmonic splines has been presented.

Table 7: Comparison study of frequency parameters, $\lambda = (\omega b^2/\pi^2)(\rho t/D)^{1/2}$ for square isotropic plates with SSSS boundaries.

t/b	Method of solution	Mode					
		(1, 1)	(1, 2)	(2, 1)	(2, 2)	(1, 3)	(3, 1)
0.01	Classical theory [4]	2.000	5.000	5.000	8.000	10.000	10.000
	FSDT, Ritz method [5]	1.999	4.995	4.995	7.998	9.981	9.981
	Orthogonal polynomials [3]	1.999	4.995	4.995	7.998	9.981	9.981
	Present, grid = 11 × 11	1.9695	5.1285	5.1286	7.9350	10.4481	10.4689
	Present, grid = 15 × 15	1.9950	5.0563	5.0563	8.0279	10.1396	10.1719
	Present, grid = 21 × 21	1.9997	5.0189	5.0189	8.0180	10.0261	10.0464
0.1	Classical theory [4]	2.000	5.000	5.000	8.000	10.000	10.000
	3D analysis [6]	1.934	4.662	4.622	7.103	8.662	8.662
	FSDT, Ritz method [5]	1.931	4.605	4.605	7.064	8.605	8.605
	Orthogonal polynomials [3]	1.931	4.605	4.605	7.064	8.605	8.605
	Present, grid = 11 × 11	1.9387	4.6608	4.6608	7.1929	8.7181	8.7134
	Present, grid = 15 × 15	1.9386	4.6448	4.6448	7.1589	8.7070	8.7134
	Present, grid = 21 × 21	1.9376	4.6394	4.6394	7.1449	8.7091	8.7110

Table 8: Comparison study of frequency parameters, $\lambda = (\omega b^2/\pi^2)(\rho t/D)^{1/2}$ for square isotropic plates with CCCC boundaries, $h/a = 0.1$.

Mode	$N = 7$	$N = 11$	$N = 15$	CPT [4]	FSDT (Ritz) [5]	Liew et al. [3]	
1, 1	3.2900	3.2478	3.2461	3.646	3.297	3.297	3.292
1, 2	6.2129	6.1577	6.1648	7.436	6.290	6.290	6.276
2, 1	6.2129	6.1577	6.1648	7.436	6.290	6.290	6.276
2, 2	8.8256	8.6192	8.6169	10.964	8.837	8.842	8.792
1, 3	9.8350	10.0951	10.1473	13.333	10.376	10.376	10.356
3, 1	9.9634	10.2240	10.2712	13.395	10.465	10.461	10.455

Through numerical experiments, the capability and efficiency of the present method for eigenvalue problems are demonstrated, and the numerical accuracy and convergence are thoughtfully examined.

When compared to other RBFs, polyharmonic splines show good stability and accuracy. However, proper modelling of plates should consider both a good numerical technique and an adequate shear deformation theory.

References

[1] R. L. Hardy, "Multiquadric equations of topography and other irregular surfaces," *Journal of Geophysical Research*, vol. 176, pp. 1905–1915, 1971.

[2] E. J. Kansa, "Multiquadrics—a scattered data approximation scheme with applications to computational fluid-dynamics—I. Surface approximations and partial derivative estimates," *Computers & Mathematics with Applications*, vol. 19, no. 8-9, pp. 127–145, 1990.

[3] K. M. Liew, K. C. Hung, and M. K. Lim, "Vibration of mindlin plates using boundary characteristic orthogonal polynomials," *Journal of Sound and Vibration*, vol. 182, no. 1, pp. 77–90, 1995.

[4] A. W. Leissa, "The free vibration of rectangular plates," *Journal of Sound and Vibration*, vol. 31, pp. 257–293, 1973.

[5] D. J. Dawe, "Buckling and vibration of plate structures including shear deformation and related effects," in *Aspects of the Analysis of Plate Structures*, pp. 73–99, Clarendon Press, Oxford, UK, 1985.

[6] S. Srinivas, "A refined analysis of composite laminates," *Journal of Sound and Vibration*, vol. 30, no. 4, pp. 495–507, 1973.

[7] E. Reissner, "A consistment treatment of transverse shear deformations in laminated anisotropic plates," *AIAA Journal*, vol. 10, no. 5, pp. 716–718, 1972.

[8] J. N. Reddy, *Mechanics of Laminated Composite Plates: Theory and Analysis*, CRC Press, Boca Raton, Fla, USA, 1997.

[9] E. Reissner and Y. Stavsky, "Bending and stretching of certain types of heterogeneous aeolotropic elastic plates," *Journal of Applied Mechanics*, vol. 28, pp. 402–408, 1961.

[10] Y. Stavsky, "Bending and stretching of laminated aelotropic plates," *Journal of Engineering Mechanics*, vol. 87, pp. 31–56, 1961.

[11] S. B. Dong, K. S. Pister, and R. L. Taylor, "On the theory of laminated anisotropic plates and shells," *Journal of Aeronautical Science*, vol. 29, no. 8, pp. 969–975, 1962.

[12] P. C. Yang, C. H. Norris, and Y. Stavsky, "Elastic wave propagation in heterogeneous plates," *International Journal of Solids and Structures*, vol. 2, no. 4, pp. 665–684, 1966.

[13] S. A. Ambartsumyan, *Theory of Anisotropic Plates*, Technomic, Stamford, Conn, USA, 1969.

[14] J. M. Whitney and A. W. Leissa, "Analysis of heterogeneous anisotropic plates," *Journal of Applied Mechanics*, vol. 36, no. 2, pp. 261–266, 1969.

[15] J. N. Reddy, "A simple higher-order theory for laminated composite plates," *Journal of Applied Mechanics, ASME Transactions*, vol. 51, no. 4, pp. 745–752, 1984.

[16] J. N. Reddy, "A refined nonlinear theory of plates with transverse shear deformation," *International Journal of Solids and Structures*, vol. 20, no. 9-10, pp. 881–896, 1984.

[17] B. N. Pandya and T. Kant, "Higher-order shear deformable theories for flexure of sandwich plates—finite element evaluations," *International Journal of Solids and Structures*, vol. 24, pp. 1267–1286, 1988.

[18] G. Akhras, M. S. Cheung, and W. Li, "Finite strip analysis of anisotropic laminated composite plates using higher-order shear deformation theory," *Computers and Structures*, vol. 52, no. 3, pp. 471–477, 1994.

[19] E. Carrera, "C^0 reissner-mindlin multilayered plate elements including zig-zag and interlaminar stress continuity," *International Journal for Numerical Methods in Engineering*, vol. 39, no. 11, pp. 1797–1820, 1996.

[20] Y. C. Hon, M. W. Lu, W. M. Xue, and Y. M. Zhu, "Multiquadric method for the numerical solution of a biphasic mixture model," *Applied Mathematics and Computation*, vol. 88, no. 2-3, pp. 153–175, 1997.

[21] Y.-C. Hon, K. F. Cheung, X.-Z. Mao, and E. J. Kansa, "Multiquadric solution for shallow water equations," *Journal of Hydraulic Engineering*, vol. 125, no. 5, pp. 524–533, 1999.

[22] J. G. Wang, G. R. Liu, and P. Lin, "Numerical analysis of Biot's consolidation process by radial point interpolation method," *International Journal of Solids and Structures*, vol. 39, no. 6, pp. 1557–1573, 2002.

[23] G. R. Liu and Y. T. Gu, "A local radial point interpolation method (LRPIM) for free vibration analyses of 2-D solids," *Journal of Sound and Vibration*, vol. 246, no. 1, pp. 29–46, 2001.

[24] J. G. Wang and G. R. Liu, "A point interpolation meshless method based on radial basis functions," *International Journal for Numerical Methods in Engineering*, vol. 54, no. 11, pp. 1623–1648, 2002.

[25] J. G. Wang and G. R. Liu, "On the optimal shape parameters of radial basis functions used for 2-D meshless methods," *Computer Methods in Applied Mechanics and Engineering*, vol. 191, no. 23-24, pp. 2611–2630, 2002.

[26] X. L. Chen, G. R. Liu, and S. P. Lim, "An element free Galerkin method for the free vibration analysis of composite laminates of complicated shape," *Composite Structures*, vol. 59, no. 2, pp. 279–289, 2003.

[27] K. Y. Dai, G. R. Liu, K. M. Lim, and X. L. Chen, "A mesh-free method for static and free vibration analysis of shear deformable laminated composite plates," *Journal of Sound and Vibration*, vol. 269, no. 3–5, pp. 633–652, 2004.

[28] G. R. Liu and X. L. Chen, "Buckling of symmetrically laminated composite plates using the element-free galerkin method," *International Journal of Structural Stability and Dynamics*, vol. 2, pp. 281–294, 2002.

[29] K. M. Liew, X. L. Chen, and J. N. Reddy, "Mesh-free radial basis function method for buckling analysis of non-uniformly loaded arbitrarily shaped shear deformable plates," *Computer Methods in Applied Mechanics and Engineering*, vol. 193, no. 3–5, pp. 205–224, 2004.

[30] Y. Q. Huang and Q. S. Li, "Bending and buckling analysis of antisymmetric laminates using the moving least square differential quadrature method," *Computer Methods in Applied Mechanics and Engineering*, vol. 193, no. 33-35, pp. 3471–3492, 2004.

[31] L. Liu, G. R. Liu, and V. B. C. Tan, "Element free method for static and free vibration analysis of spatial thin shell structures," *Computer Methods in Applied Mechanics and Engineering*, vol. 191, no. 51-52, pp. 5923–5942, 2002.

[32] A. J. M. Ferreira, "A formulation of the multiquadric radial basis function method for the analysis of laminated composite plates," *Composite Structures*, vol. 59, no. 3, pp. 385–392, 2003.

[33] A. J. M. Ferreira, "Thick composite beam analysis using a global meshless approximation based on radial basis functions," *Mechanics of Advanced Materials and Structures*, vol. 10, no. 3, pp. 271–284, 2003.

[34] A. J. M. Ferreira, C. M. C. Roque, and P. A. L. S. Martins, "Analysis of composite plates using higher-order shear deformation theory and a finite point formulation based on the multiquadric radial basis function method," *Composites Part B*, vol. 34, no. 7, pp. 627–636, 2003.

[35] A. J. M. Ferreira, C. M. C. Roque, and R. M. N. Jorge, "Free vibration analysis of symmetric laminated composite plates by FSDT and radial basis functions," *Computer Methods in Applied Mechanics and Engineering*, vol. 194, no. 39–41, pp. 4265–4278, 2005.

[36] L. M. J. S. Dinis, R. M. Natal Jorge, and J. Belinha, "Analysis of plates and laminates using the natural neighbour radial point interpolation method," *Engineering Analysis with Boundary Elements*, vol. 32, no. 3, pp. 267–279, 2008.

[37] P. Xia, S. Y. Long, H. X. Cui, and G. Y. Li, "The static and free vibration analysis of a nonhomogeneous moderately thick plate using the meshless local radial point interpolation method," *Engineering Analysis with Boundary Elements*, vol. 33, no. 6, pp. 770–777, 2009.

[38] P. Zhu and K. M. Liew, "Free vibration analysis of moderately thick functionally graded plates by local Kriging meshless method," *Composite Structures*, vol. 93, no. 11, pp. 2925–2944, 2011.

[39] L. M. J. S. Dinis, R. M. N. Jorge, and J. Belinha, "Static and dynamic analysis of laminated plates based on an unconstrained third order theory and using a radial point interpolator meshless method," *Computers and Structures*, vol. 89, no. 19-20, pp. 1771–1784, 2011.

[40] B. Chinnaboon, S. Chucheepsakul, and J. T. Katsikadelis, "A BEM-based domain meshless method for the analysis of Mindlin plates with general boundary conditions," *Computer Methods in Applied Mechanics and Engineering*, vol. 200, no. 13–16, pp. 1379–1388, 2011.

[41] K. M. Liew, X. Zhao, and A. J. M. Ferreira, "A review of meshless methods for laminated and functionally graded plates and shells," *Composite Structures*, vol. 93, no. 8, pp. 2031–2041, 2011.

[42] J. Belinha, L. M. J. S. Dinis, and R. M. Natal Jorge, "The natural radial element method," *International Journal for Numerical Methods in Engineering*, vol. 93, no. 12, pp. 1286–1313, 2013.

[43] W. R. Madych and S. A. Nelson, "Multivariate interpolation and conditionally positive definite functions—II," *Mathematics of Computation*, vol. 54, no. 189, pp. 211–230, 1990.

[44] J. Yoon, "Spectral approximation orders of radial basis function interpolation on the Sobolev space," *SIAM Journal on Mathematical Analysis*, vol. 33, no. 4, pp. 946–958, 2001.

[45] H. Wendland, "Error estimates for interpolation by compactly supported radial basis functions of minimal degree," *Journal of Approximation Theory*, vol. 93, no. 2, pp. 258–272, 1998.

[46] M. D. Buhmann, "Radial basis functions," *Acta Numerica*, vol. 9, pp. 1–38, 2000.

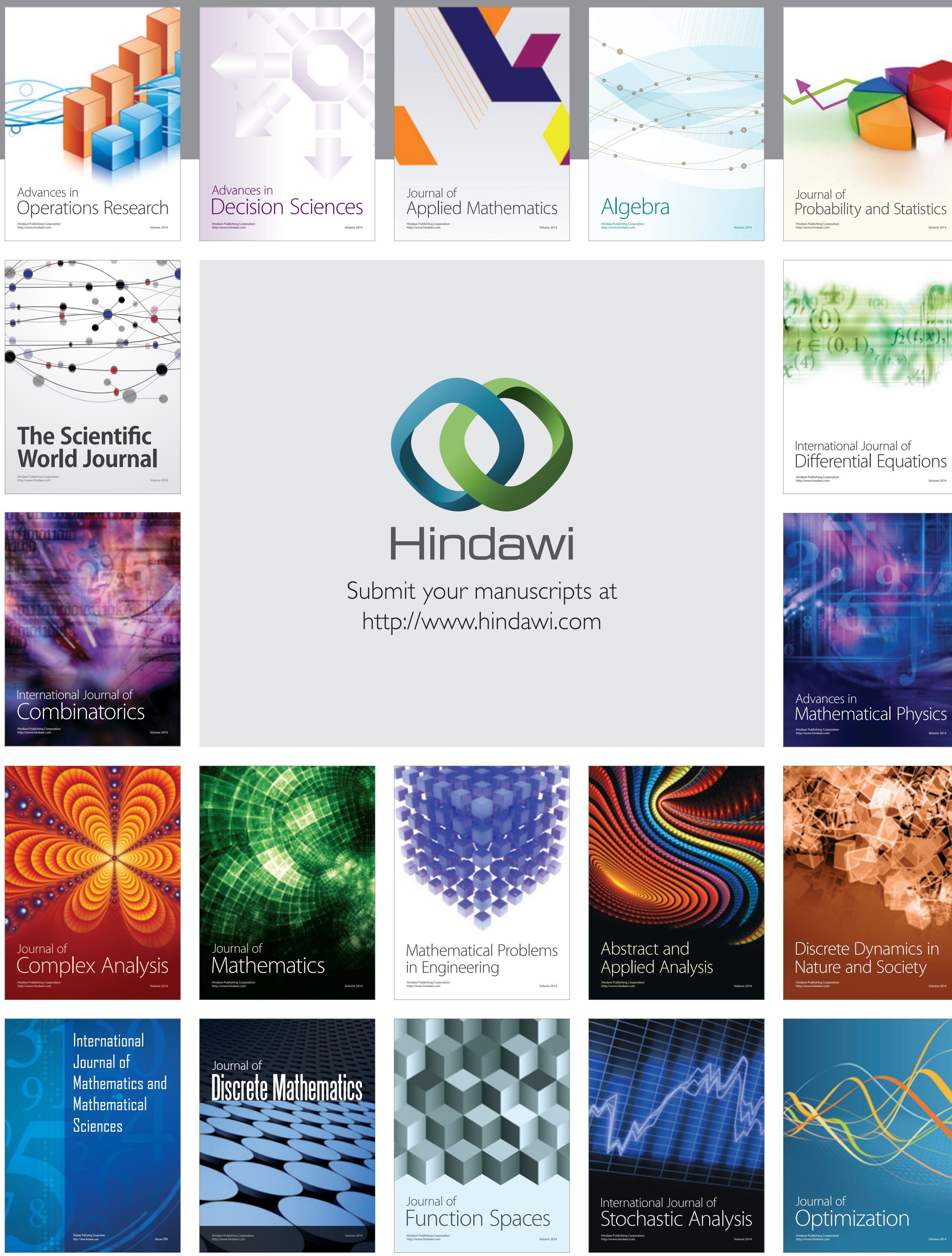
Advances in
Operations Research
Advances in
Decision Sciences
Journal of
Applied Mathematics
Algebra
Journal of
Probability and Statistics
The Scientific
World Journal
International Journal of
Differential Equations
Hindawi
Submit your manuscripts at
http://www.hindawi.com
International Journal of
Combinatorics
Advances in
Mathematical Physics
Journal of
Complex Analysis
Journal of
Mathematics
Mathematical Problems
in Engineering
Abstract and
Applied Analysis
Discrete Dynamics in
Nature and Society
International
Journal of
Mathematics and
Mathematical
Sciences
Journal of
Discrete Mathematics
Journal of
Function Spaces
International Journal of
Stochastic Analysis
Journal of
Optimization